JOURNAL OF MATERIALS SCIENCE 20 (1985) 1301–1309

Nonlinear diffusion in spinodal decomposition: a numerical solution

T. TSAKALAKOS
Department of Mechanics and Material Science, Rutgers University, P.O. Box 909, Piscataway, New Jersey 08854, USA

M. P. DUGAN
RCA Solid State Technology Center, Route 202, Somerville, New Jersey, USA

The numerical solution of the one-dimensional nonlinear diffusion equation with a negative diffusion coefficient (up-hill diffusion) by a five-point approximation central difference scheme is considered. The stability criteria are discussed in detail and a numerical solution is provided for a specific case in which the time evolution of a periodic composition wave is presented with growth eventually leading to a stationary configuration. A critical comparison of the numerical solution with existing analytical solutions is shown. This leads to a simple semi-empirical growth law for studying the kinetics of spinodal decomposition in alloys.

1. Introduction

In recent years, a new class of material, the spinodal alloys [1, 2], have shown some unusual properties that have generated considerable interest in the field of materials science and engineering. An important factor for the current excitement in the field is the fact that the excellent properties of these alloys, such as mechanical, magnetic, electrical, etc, are a direct consequence of their microstructure which is produced by a solid phase transformation called spinodal decomposition. In a system like a spinodal alloy, certain compositional fluctuations are stable with respect to the solid solution and grow. Such a growth of composition wave is usually accompanied by a static lattice modulation which in turn produces internal stresses. Because of the anisotropic nature of the elastic strain energy associated with the internal stresses, the microstructure at the early stage of the decomposition consists of the three mutually perpendicular composition waves along the three ⟨1 0 0⟩ directions of the cubic materials in which spinodal decomposition is usually observed. Perhaps part of the considerable amount of interest that was shown to spinodal decomposition, resulted from the fact that a very elegant and mathematically attractive theory was developed in the early sixties that could account for most of the experimental observations on these alloys. Cahn [3, 4] developed a generalized diffusion equation that explained the growth of the composition waves and their crystallographic orientation. The solution of the diffusion equation by Cahn predicted an exponential growth rate and is valid only for the very early stages, i.e. for infinitesimal fluctuations. This solution fails to describe the time evolution of the microstructure at long times. In a number of subsequent [5, 6] investigations of the later stages of the spinodal decomposition, some qualitative observations have been provided as to how a composition wave of large amplitude will grow. Most of the investigations state that at later stages the system spends most of its time in configurations which are called stationary states. These states are periodic waves of certain shape and amplitude depending on the wavelength and are solutions of the time-independent nonlinear diffusion equation. Recently, Tsakalakos [7] has shown that the analytical expressions of the stationary states in a one-dimensional system are Jacobian elliptic functions.

Despite the success of the linear theory in describing the early stages of spinodal decomposition

0022–2461/85 $03.00 + .12

and the analytical solutions for the stationary states there are no current data that actually link the infinitesimal periodic wave with its corresponding stationary state. Nor has there been any quantitative growth rate derived at intermediate and later stages of the decomposition. Perturbation techniques [7] have shown there is a "slow down" effect from the exponential growth rate of the linear regime when the system approaches its stationary state. It is the purpose of this paper to provide an exact numerical solution of the nonlinear diffusion equation in order to obtain time evolution of a spinodal structure. The generalized diffusion equation in one-dimension as derived by Cahn [3, 4] is given by

$$\frac{\partial u}{\partial t'} = \frac{\partial}{\partial x'}\left(\tilde{D}\frac{\partial}{\partial x'}u\right) - 2\tilde{K}\frac{\partial^4 u}{\partial x'^4}, \qquad (1)$$

where $u(x, t) = c(x, t) - c_0$, in which $c(x, t)$ is the composition at the distance x and at time t and c_0 is the average composition of the binary alloy, $\tilde{D}$ is the interdiffusion coefficient which in general for large amplitudes, depends on the composition, and the last term in the diffusion equation is called "gradient" energy term and was introduced by Cahn and Hilliard [8] to account for the increase of the free energy due to the gradient of composition. Equation 1 can be normalized by the following substitutions:

$$x' = lx, \quad t' = 4\tilde{K}t \text{ and } l = 2\tilde{K}^{1/2},$$

yielding

$$\frac{\partial u}{\partial t} = \frac{\partial}{\partial x}\left(\tilde{D}\frac{\partial}{\partial x}u\right) - \frac{1}{2}\frac{\partial^4 u}{\partial x^4}. \qquad (2)$$

In order to maintain nonlinear terms up to the fourth order in this differential equation, a quadratic dependence of $\tilde{D}$ on the composition variation is required:

$$\tilde{D} = D_0 + D_1 u + D_2 u^2,$$

for the case with $D_0 < 0$, $D_1 = 0$, $D_2 > 0$ and $\nu = D_2/|D_0|$ we obtain the reduced equation

$$\frac{\partial u}{\partial t} = D_0\frac{\partial}{\partial x}\left[(-1 + \nu u^2)\frac{\partial u}{\partial x}\right] - \frac{1}{2}\frac{\partial^4 u}{\partial x^4}. \qquad (3)$$

Since the solution is periodic with wavelength, λ, the initial and boundary conditions are:

$$u(x, 0) = Q\cos 2\pi x/\lambda \qquad (4a)$$

and

$$\frac{\partial u}{\partial x}(0, t) = \frac{\partial u}{\partial x}(\lambda, x) = 0, \quad t > 0, \qquad (4b)$$

where Q is the amplitude of the composition wave.

2. Central difference scheme

The general approach to solving differential equations by numerical methods requires the definition of intervals along the x-axis. The value of the derivative in each interval is then approximated by a straight line. The mean value theorem states that a straight line connecting two points on a curve is parallel to the derivative of at least one point on the included interval. For slowly varying functions, this point is in the centre of the interval and the derivative is approached as the interval is made smaller. Taylor's expansion about the central point provides the numerical expressions and estimates the errors. The three-point central difference scheme uses the neighbouring points on both sides of the central point, the five-point scheme uses two points on both sides.

The Appendix contains a detailed error analysis for our model. At this point, it is sufficient to state that the truncation or round-off error introduced during any step in the iteration process must decay with subsequent iterations rather than grow in order that the numerical solution be stable and approach the analytical solution.

In order to demonstrate the fundamental difficulty that one faces in attempting to obtain a numerical solution for the diffusion equation given in Equation 3, let us assume that $\nu = 0$ and $K = 0$. In this case, the equation reduces to:

$$\frac{\partial u}{\partial t} = -|D_0|\frac{\partial^2 u}{\partial x^2}. \qquad (5)$$

This equation is identical to the backward heat diffusion equation better known as "ill-posed problems" in heat conduction.

The three-point approximation to the second derivative about point x_0 is:

$$\frac{\partial^2 u}{\partial x^2} = (1/\Delta x^2)[u(x_0 - \Delta x) - 2u(x_0) + u(x_0 + \Delta x)].$$

By separating terms with respect to space and time and rearranging, Equation 5 can be written as:

$$u_i^{j+1} = -r(u_{i+1}^j + u_{i-1}^j) + (1 + 2r)u_i^j \qquad (6)$$

where $r = \Delta t/\Delta x^2$, i and j refer to this discretization operation in space and time, respectively. As $(1 + 2r) \geqslant 1$ in the last term, we cannot ensure convergence of the numerical model with the analytical solution. Indeed, our attempts to obtain a solution by this method produced unstable results.

Because of this instability, the method of finite differences employing a five-point formula based on Taylor series expansion about x_0 was selected. The spatial partial derivatives are expressed using the central difference scheme:

$$u'(x_0) = 1/12\Delta x[u(x_0-2\Delta x)-8u(x_0-\Delta x) + 8u(x_0+\Delta x)-u(x_0+2\Delta x)] \quad (7a)$$

$$u''(x_0) = 1/12\Delta x^2[-u(x_0-2\Delta x) + 16u(x_0-\Delta x_0)-30u(x_0) + 16u(x_0+\Delta x)-u(x_0+2\Delta x)]. \quad (7b)$$

$$u^{IV}(x_0) = 1/\Delta x^4[-u(x_0-2\Delta x) - 4u(x_0-\Delta x)+6u(x_0) - 4u(x_0+\Delta x)+u(x_0+2\Delta x)]. \quad (7c)$$

The following truncation error terms are associated with each of these expressions:

$$E_I = \frac{\Delta x^4}{90}[u^v(\xi)-u^v(\eta)] \quad (8a)$$

$$E_{II} = \frac{\Delta x^3}{30}[2u^v(\xi)-u^v(\eta)] \approx \frac{x^3}{30}u^v(\eta) \quad (8b)$$

$$E_{IV} = \frac{\Delta x}{15}[u^v(\xi)-8u^v(\eta)] \approx -\frac{7}{15}\Delta x u^v(\eta), \quad (8c)$$

where u^v is the fifth derivative of u, Δx is a uniform interval along the x-axis and η and ξ are points within the interval. A discussion of the error analysis is included in the Appendix.

The partial derivative with respect to time is expressed as the forward difference:

$$\frac{\partial u(x,t)}{\partial t} = \frac{1}{\Delta t}[u(x,t+\Delta t)-u(x,t)]. \quad (9)$$

Thus, if we discretize in space, using the five-point central differences for the derivatives, a system of ordinary differential equations is obtained, which after time discretization by forward differences gives:

$$U_i^{j+1} = AU_i^j \quad j=0,1,2,3,\ldots,N$$

where

$$U_i^j = [u_0^j, u_1^j, u_2^j \ldots, u_n]^T$$

$$A = \begin{pmatrix} F_0 & F_1 & F_2 & 0 & 0 & 0 & 0 & & & & 0 & F_2 & F_1 & 0 \\ F_1 & F_0 & F_1 & F_2 & 0 & 0 & 0 & & & & 0 & 0 & F_2 & 0 \\ F_2 & F_1 & F_0 & F_1 & F_2 & 0 & 0 & & & & 0 & 0 & 0 & 0 \\ 0 & F_2 & F_1 & F_0 & F_1 & F_2 & 0 & & & & & & & \\ & & & & & & & \cdots & & & & & & \\ & & & & & & & & & & & & & \\ 0 & 0 & 0 & 0 & & & & & & & 0 & F_2 & F_1 & F_0 & F_1 & F_2 & 0 \\ 0 & F_2 & 0 & 0 & & & & & & & 0 & 0 & F_2 & F_1 & F_0 & F_1 & F_2 \\ 0 & F_1 & F_2 & 0 & & & & & & & 0 & 0 & 0 & F_2 & F_1 & F_0 & F_1 \\ & & & & & & & & & & 0 & 0 & 0 & 0 & F_2 & F_1 & F_0 \end{pmatrix}, \quad (10)$$

where N is the number of time iterations, n is the number of discrete intervals in space along one period of the composition wave and F_i, $i=0,1,2$ are not constants but nonlinear functions of U_i^js given by:

$$F_0 = 1-r\left(\frac{5}{2}\tilde{D}+\frac{3}{\Delta x^2}-2\nu U'^2\right) \quad (11a)$$

$$F_1 = r\left(\frac{4}{3}\tilde{D}+\frac{2}{\Delta x^2}\right) \quad (11b)$$

$$F_2 = -r\left(\frac{\tilde{D}}{12}+\frac{1}{2\Delta x^2}\right) \quad (11c)$$

where

$$r = \frac{\Delta t}{\Delta x^2}, \quad \tilde{D} = -1+\nu(U_i^j)^2$$

and

$$U'^2 = \left(\frac{\partial U}{\partial x}\right)^2 = \frac{1}{144\Delta x^2}(U_{i-2}-8U_{i-1} + 8U_{i+1}-U_{i+2})^2.$$

A has the characteristics of a transfer function,

that is, a function which transfers the values of the composition variation at time interval U_i^j into the value at the next time interval U_i^{j+1}.

It should be emphasized that the matrix elements of A are not constants but functions of the composition variations U_i^j. Such a pseudo-linear representation of the nonlinear diffusion equation has a significant advantage for it assists in developing the criteria for stability and convergence. Although the coefficients of this linear representation are not constant as indicated in Equations 11a to c fruitful information can be obtained as a direct result of the physical behaviour of the nonlinear solution throughout its time evolution. By direct inspection of the nonlinear diffusion Equation 3, the following important conclusions about its solution can be stated:

1. any periodic solution cannot have amplitude larger than the $\Delta c_e = c_e - c_0$ where c_e is the equilibrium concentration. Since u is normalized to Δc_e we therefore have the condition $|U| \leqq 1$. This also implies that

$$-1 \leqq \tilde{D} \leqq -1 + \nu;$$

2. analytical solutions of the time-independent equation has shown [6–8] that the maximum slope of any periodic configuration cannot exceed the slope of the equilibrium interface which can be described by a hyperbolic tangent. In our reduced representation, Equation 5, we have the condition that: $|U'| \leqq 1$ with equality occurring for a stationary state of infinite wavelength at $x = \lambda/4$.

Based upon these two physical conditions, we can now conclude that the F_is are bounded quantities for a given choice of the spatial and time intervals of the discretization.

3. Results and discussion

In order to test the stability of the numerical scheme the following non-linear case was chosen for investigation. A sinusoidal composition fluctuation was assumed as the initial condition at $t = 0$ for the profile of the composition wave, having the following characteristic values:

$$t = 0 \quad U = 0.1 \cos 2\pi x/\lambda; \; \lambda = 16.142\,664.$$

A spatial discretization of 80 intervals was assigned and the following values of the numerical parameters were chosen which satisfied the stability criterion given in Equation A6.

$$\Delta t = 0.000\,25, \quad \Delta x = 0.201\,7833$$

which gives a value for $r = 0.00614$.

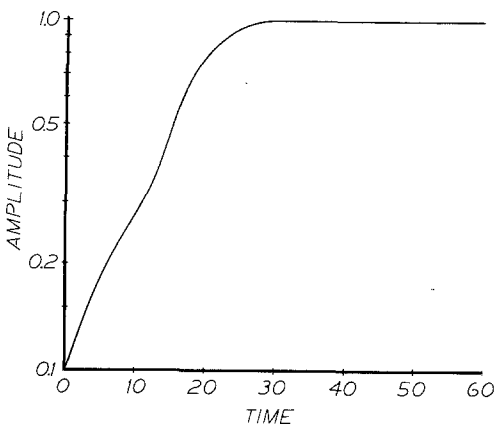

Figure 1 Growth of the composition wave. The amplitude increases exponentially in the early stages, behaves nonlinearly in the intermediate stage showing a slow-down effect. At later stages a stationary state is reached.

Fig. 1 shows the time evolution of the composition wave. It can be seen from the semi-logarithmic plot that the amplitude of the wave increases exponentially in the early stages as predicted by the linear theory. For intermediate stages the wave behaves nonlinearly by showing a "slow-down" effect followed by rapid growth. At later stages the growth diminishes and the wave reaches a stationary state. No further growth is observed.

The results of these numerical calculations verify the prediction of early work [6–8], that is, in real alloy systems the composition waves spend most of the time in configurations which are stationary states of the time independent ($du/dt = 0$) nonlinear diffusion equation. Tsakalakos [7] has shown that the stationary states can be expressed by:

$$U^*(x) = (1-\mu^2)^{1/2} \operatorname{sn}[(1+\mu^2)^{1/2}x], \quad (12)$$

where the asterisk indicates that $U(x)$ is a stationary state and μ is a parameter taking values between 0 and 1. The $\operatorname{sn}(z)$ is the Jacobian Elliptic function and is periodic with wavelength:

$$\lambda = \frac{4}{(1+\mu^2)^{1/2}} \kappa(k^2) \quad (13)$$

where $k^2 = (1-\mu^2)/(1+\mu^2)$ and K is the complete elliptic integral of the first kind. If $\mu = 0$ then

$$U^* = \tanh x \quad (14)$$

and for $\mu \to 1$ it can be shown that

$$U^*_{\mu \to 1} \cong (1-\mu^2)^{1/2} \sin 2^{1/2}x. \quad (15)$$

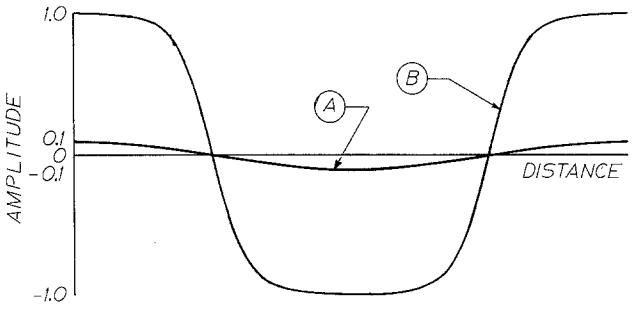

Figure 2 Profile of a single wavelength. The initial profile A at $t = 0$ and the numerical and analytical square-like wave B at $t = 60$.

For the intermediate case, the stationary states approach square-like waves. For our particular case the wavelength $\lambda = 16.142\,664$ corresponds to $k^2 = 0.995$ for which the amplitude of the stationary states can be calculated from Equation 14 to be:

$$Q^*_{\text{th}} = 9987$$

The numerical solution provided an amplitude:

$$Q_{\text{cal}} = 0.9984,$$

which is in remarkable agreement with the theoretical value.

The profile of the wave is shown in Fig. 2. The initial profile at $t = 0$ is shown in curve A and the numerical solution is plotted at $t = 60$ (240 000 iterations) together with the analytical solution (curve B). It is seen that the numerical and analytical solution agree to a better accuracy than 0.03%.

In order to compare the growth rate of the numerical solution with that predicted by the linear theory, a Fourier transform of the computed composition profile was performed every 1000 iterations. According to the linear theory the growth rate is given by:

$$R(k) = k^2\left(-1 + \frac{k^2}{2}\right), \qquad (16)$$

and for the above studied wavelength:

$$R = 0.140\,023.$$

Thus, at $t = 0$, the Fourier amplitude should grow according to:

$$Q(t) = 0.1e^{0.140\,023t}.$$

In Fig. 1, the amplitude of the first Fourier component is plotted against time as calculated by a numerical Fourier transform of the computed profile. It is that the wave increases exponentially at the early stages with growth rate $R = 0.140$ which is in excellent agreement with the theoretical calculations. At later stages the growth rate of the Fourier amplitude decreases continuously and finally reaches the value $Q^* = 1.18$. To compare this value with the expected one, we expand the stationary states given in Equation 12 in Fourier series [9]:

$$U^* = (2\pi(1+\mu^2)^{1/2}/\kappa) \times \sum_{m=0}^{\infty} \{q^{(m+1)/2}/[1-q^{(2m+1)}]\} \times \sin[(2m+1)\pi u/2\kappa] \qquad (17)$$

where

$$q = \exp(-\pi\kappa'/\kappa), \quad \kappa' \equiv \pi(1-k^2).$$

For $k^2 = 0.995$, the amplitude of the first Fourier component in this expansion becomes: $Q^* = 1.18$ which is identical to the one that the wave reaches at the very late stages.

Perhaps the most important point in these numerical computations is the fact that the numerical scheme provides the actual kinetics from the early exponential growth to the later stages where a gradual retardation occurs and the wave reaches its stationary state. Although the analytical solutions exist for both the very early stages and the stationary state (infinite time) there has been no solution that links the two extreme cases together. Nor has there been any kinetics study of the intermediate configurations.

Tsakalakos [7] has derived an approximate analytical formula for time evolution of the spinodal structure. This formula was based on perturbation techniques and is given by:

$$Q(t) = Q_1^* \tanh[(Q_0/Q_1^*)e^{R(k)t}]. \qquad (18)$$

This approximate solution is plotted in Fig. 3 as curve B together with the numerical solution

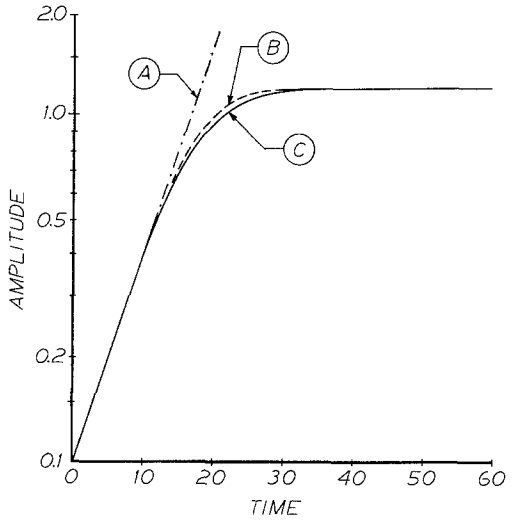

Figure 3 The increase in amplitude of the composition wave against time. Curve A represents Cahn's linear solution, B is Tsakalakos' approximate solution, and C is the solution by our numerical model.

(curve C) and the linear solution (curve A). It can be seen that the agreement is remarkably good and indicates why Equation 1 provides the basis for kinetics studies of spinodal alloys. Such studies have been made by Ditchek and Schwartz [2] for the Cu–9Ni–6Sn spinodal alloys. It should be finally noted that non-linear behaviour at intermediate stages ($t \sim 10$) is due to the fact that the wave is trying to assume its square-like configuration by faster growth of the higher harmonics. This is indeed observed by the numerical Fourier transform performed during the numerical solution. After this intermediate stage, the wave grows towards its stationary state.

A simulation of concentration wave growth in a spinodal alloy was performed be defining the initial concentration profile as the summation of 80 cosinusoidal waves. The amplitude of each component was set equal to 0.005 on a normalized scale. This concentration profile was discretized into 160 intervals and operated upon by the difference equation obtained by substituting Equation 7 into Equation 3.

Figs. 4 to 6 illustrate three stages in the evolution of the spinodal structure. The concentration is plotted against distance for three values of elapsed time (iterations of the programme). In Fig. 4 an early stage is illustrated which shows that the initital distribution has not been altered significantly after 10 000 iterations. Fig. 5 shows a time corresponding to an intermediate stage where the spinodal wavelength is becoming established.

The stationary state is illustrated in Fig. 6. The wave has grown in amplitude and assumed a square-like profile. A careful examination of this reveals that the profile is not exactly periodic but that there is a slight deviation from the Jacobian elliptic function mentioned in Equation [12]. The computer simulation was continued to a total of 100 000 iterations without a change in the amplitude and wavelength of Fig. 6.

An alternate approach to illustrating the growth of the concentration wave is depicted in Fig. 7. Here the amplitude as a function of time in a logarithmic scale is plotted for three positions. The exponential growth, predicted by the linear theory, does not begin at all positions simultaneously but proceeds only after the spinodal wavelength has been established. By allowing certain Fourier components to grow and others to decay, the system "sorts out" the proper wavelength for spinodal growth. The amplitude of the concentration waves begins to level off at 30 000 iterations and is nearly constant after 40 000. This transition from exponential growth to a wave of constant amplitude or the stationary state is the slow down effect predicted by the nonlinear theory [7].

In addition to the profile analysis in real space, a Fourier transform of the profile was performed at several time intervals. The increase in the

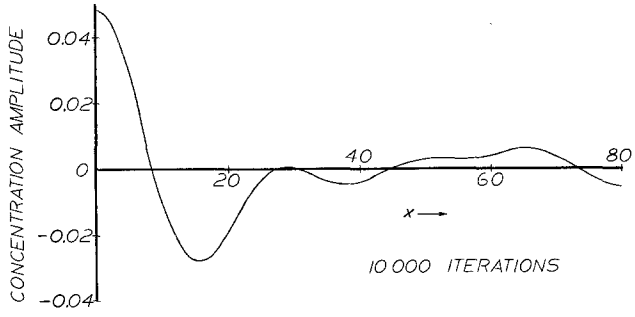

Figure 4 The composition profile at an early stage. The profile has not been altered significantly from an initial distribution composed of 80 cosinusoidal waves, each with a normalized amplitude of 0.005.

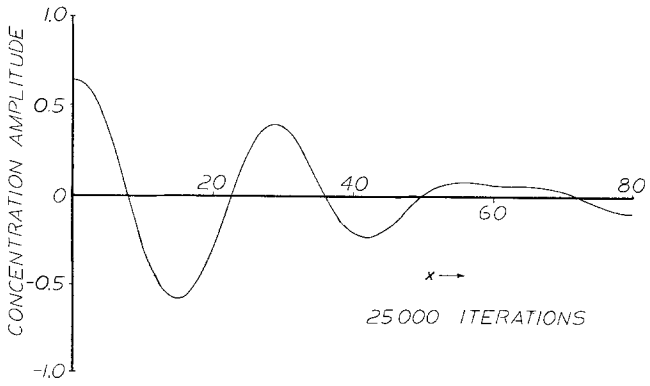

Figure 5 The composition profile at an intermediate stage where the spinodal wavelength is being established.

amplitude of three Fourier components is shown in Fig. 8. The growth obeys the predictions of the nonlinear theory of spinodal decomposition in that it is initially exponential and begins to level off as time progresses. The wave number (k = 2.8) associated with the maximum amplitude has the greatest Fourier amplitude. The wave number (k = 1.45) associated with a larger wavelength has a smaller stationary state amplitude and takes a longer time to reach it. This corresponds to the establishment of the square-like profile of the Jacobian elliptic function which requires the inclusion of additional Fourier components.

Fig. 9 depicts the increase in intensity as a function of wave number with time. The slow down effect is clearly evident as well as the shift to longer wavelengths of the real intensity as the stationary state is reached. Another feature to note is the growth of small peaks at smaller wave numbers. These are the result of computational errors and the finite size of the interval being considered in our model.

Therefore, we have demonstrated that the five-point central difference numerical scheme can be successfully employed to solve the non-linear diffusion equation particularly in the case of uphill diffusion (negative diffusion coefficient). On the practical side, this scheme provides an excellent method of studying and predicting the properties of spinodal alloys as their superior properties depend on the microstructure which, in turn, is developed through the nonlinear diffusion process. A rigorous approach to the solution of this problem will require the numerical solution of the three-dimensional nonlinear diffusion equation. In addition, a modification of initial conditions is necessary to allow for a more realistic distribution of infinitesimal composition fluctuations.

Such an attempt is currently in progress. Nevertheless, our present investigation has set forward the basis for such future development by clearly demonstrating the stability of the numerical scheme and, in general, the potentiality it has for solving more complex nonlinear problems.

Appendix . Error analysis

The error analysis of the numerical solution is based on the equation [10–12]

$$e^{j+1} = Ae^{j} \qquad \text{(A1)}$$

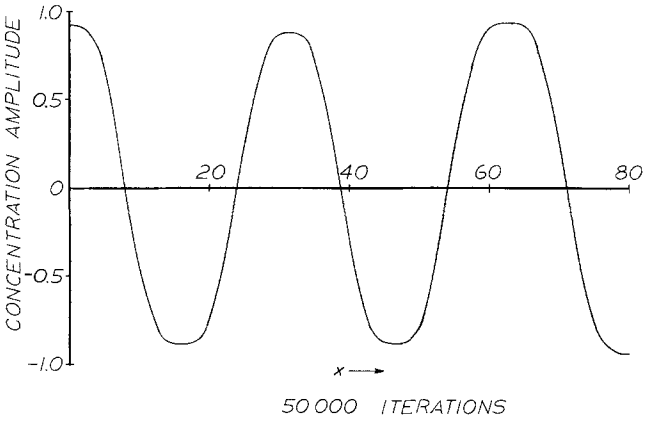

Figure 6 The composition profile at the final stage. The wave has grown in amplitude and assumed a square-like profile. The stationary state has been reached.

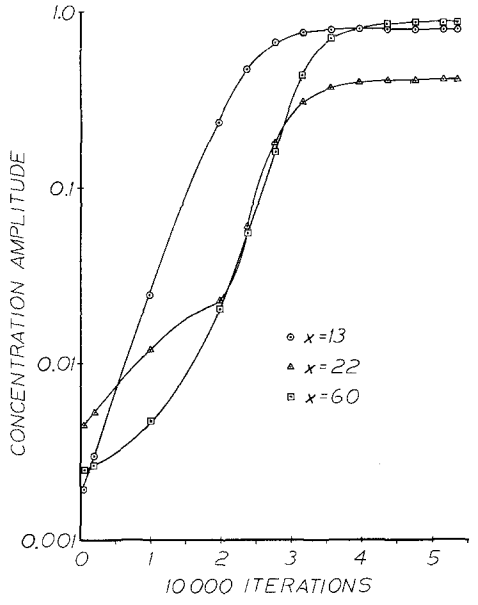

Figure 7 Amplitude as a function of time illustrating exponential growth occurring only after the spinodal wavelength is established as well as the slow-down effect and the stationary states at three positions. These positions correspond to points along the x-axis in Figs. 4 to 6.

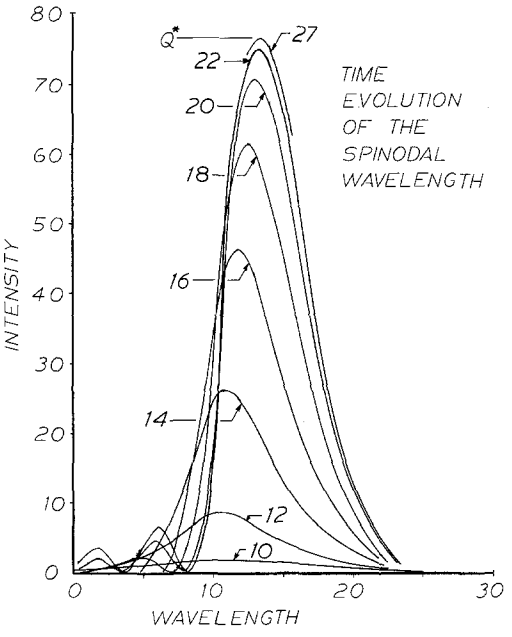

Figure 9 Time evolution of the spinodal wavelength showing increase in intensity as a function of wavelength. The slow-down effect is clearly evident as well as a shift to longer wavelengths as the stationary state (Q^*) is reached.

where $e^j = U^j - u^j$ where U_i is the exact solution and u^i is the numerical solution of the jth time interval and the quasi-pentadiagonal matrix A is given by Equation 10. To secure stability for the numerical scheme the following condition must be satisfied:

$$\rho(A) \leqslant 1,$$

where $\rho(A)$ is the spectral radius of A:

$$\rho(A) = \max |\lambda_i|,$$

where λ_i are the eigenvalues of A.

Bounds of the eigenvalues of A can be obtained using Gersgorin's theorem. Thus, we have:

$$|\lambda_i - F_0| \leqq 2|F_1| + 2|F_2|. \qquad \text{(A2)}$$

This condition is identical to the one obtained by utilizing the maximum norm condition:

$$\|e^{j+1}\| \leqq \|A\| \, \|e^j\|, \qquad \text{(A3)}$$

in which $\|A\|_\infty \leqslant 1$ is sufficient to insure stability.

$$\|A\|_\infty = |F_0| + 2|F_1| + 2|F_2| \leqq 1 \qquad \text{(A4)}$$

For $F_0 > 0$ the maximum norm is given:

$$\|A\|_\infty = 1 + r\left[\frac{\tilde{D}}{3} + \frac{2}{\Delta x^2} + 2\nu U'^2\right]. \qquad \text{(A5)}$$

This is a severe condition and for large values of U ($U > 1$) is not satisfied for any r and Δx. Despite the fact that the maximum norm condition is not met, stability was observed in the numerical

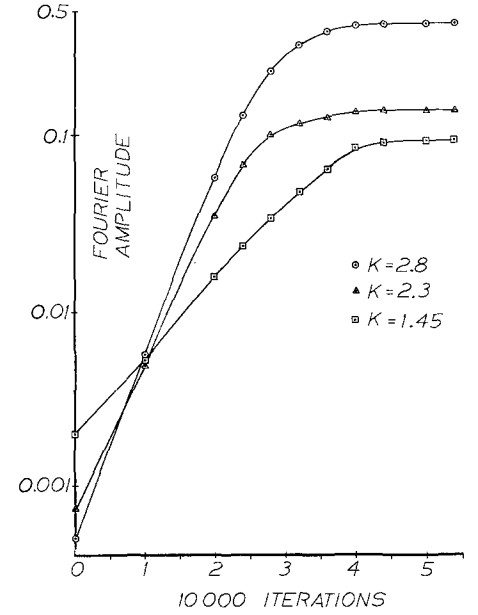

Figure 8 Growth of three Fourier components show exponential growth at early stages which levels off as time progresses.

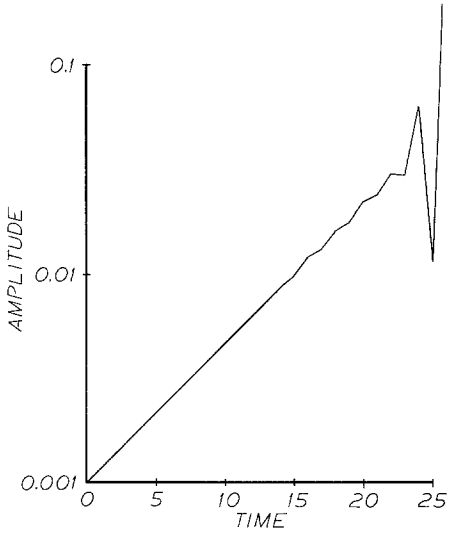

Figure 10 The effect of instabilities in the numerical model on the increase in amplitude. The stability criteria dictates that the errors due to central difference approximation and the truncation which occurs at each step must decay with each subsequent iteration rather than accumulate.

scheme if the condition $F_0 > 0$ was satisfied. For $F_0 < 0$ instability set in almost immediately after a few time steps. This is shown in Fig. 10 where the amplitude of the wave as a function of time is plotted. For the values $(r, \Delta x)$ which give $F_0 > 0$ an exponential growth is observed (the linear equation was used, $v = 0$ to compare the numerical solution to the analytical one) over three orders of magnitude of the amplitude growth.

The numerical solution is in excellent agreement with the analytical one as shown in Fig. 3. For r and Δx which give $F_0 < 0$ an error growth was observed which lead to an instability as seen in Fig. 10. Various values of r and Δx were also used and verified that the stability criterion $F_0 > 0$ was giving a stable solution. This, the condition for stability is:

$$r \leqq 1 \Big/ \left(\frac{5}{2}\tilde{D} + \frac{3}{\Delta x^2} + 2vU'^2 \right) \qquad \text{(A6)}$$

For $v = 3$ and based upon the limits of $\tilde{D}$ and U' given in Equation 11, we can determine the region of r and Δx for which stability is observed in the five-point central difference numerical scheme, as shown in Fig. 11. This pattern of behaviour for which stability is observed if the inequality A6 is met but $\|A\|_\infty > 1$, is not unexpected due to the fact the spectral radius $\rho(A)$ might be less than one, while the maximum norm is greater than one. The condition $\|A\| \leqslant 1$ is a

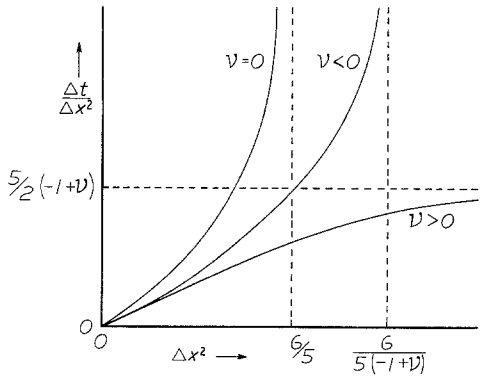

Figure 11 Graphical illustration of the stability criteria. Refer to text for details.

sufficient condition and is necessary. It should be noted that it is possible to refine the bound in Equation A2 by applying similarity transformations on A and using Gersgorin's theorem. It is also possible to perform a reduction of the original quasi-pentadiagonal matrix A to a symmetric tri-diagonal matrix using Given's or Householder's method for matrix reductions [13]. In such a symmetric tri-diagonal form, Sturm's sequence property can be applied to refine the bounds of the eigenvalues and thus provide a better approximation to the spectral radius $\rho(A)$.

References

1. J. E. HILLIARD, "Phase Transformations", edited by H. I. Aaronson, (American Society of Metals, Metals Park, Ohio, 1970), pp. 497–556.
2. B. DITCHEK and L. H. SCHWARTZ, *Ann. Rev. Mater. Sci.* 9 (1979) 219.
3. J. W. CAHN, *Acta Metall.* 9 (1961) 795.
4. *Idem, ibid.* **10** (1962) 179.
5. *Idem, ibid.* **14** (1966) 1685.
6. J. S. LANGER, *Ann. Phys.* **65** (1971) 53.
7. T. TSAKALAKOS, PhD thesis, Northwestern University Evanston, Illinois (1977).
8. J. W. CAHN and J. E. HILLIARD, *J. Chem. Phys.* 28 (1958) 25.
9. I. S. GRADSHTEYN and I. M. RYZHIK, "Table of Integrals, Series and Products" (Academic Press, New York, 1965).
10. J. L. SIEMIENIUCH and I. GLADWELL, *Int. J. Num. Meth. Engng.* **12** (1978) 899.
11. D. F. GRIFFITHS, I. CHRISTIE and A. R. MITCHELL, *ibid.* **15** (1980) 1075.
12. C. F. GERALD, "Applied Numerical Analysis", (Addison-Wesley, Reading, Massachusetts, 1978) pp. 392–416.
13. J. H. WILKINSON, "Algebraic Eigenvalue Problem" (Oxford University Press, Oxford 1965).

Received 1 June
and accepted 4 June 1984